Entanglement in the classical limit: Quantum correlations from classical probabilities

A. Matzkin

LPTM (CNRS Unité 8089), Université de Cergy-Pontoise, F-95302 Cergy-Pontoise Cedex, France

(Received 24 January 2011; published 24 August 2011)

We investigate entanglement for a composite closed system endowed with a scaling property which allows the dynamics to be kept invariant while the effective Planck constant $\hbar_{\rm eff}$ of the system is varied. Entanglement increases as $\hbar_{\rm eff} \to 0$. Moreover, for sufficiently low $\hbar_{\rm eff}$ the evolution of the quantum correlations, encapsulated, for example, in the quantum discord, can be obtained from the mutual information of the corresponding classical system. We show this behavior is due to the local suppression of path interferences in the interaction that generates the entanglement.

DOI: 10.1103/PhysRevA.84.022111 PACS number(s): 03.65.Ta, 03.65.Sq, 03.67.Mn, 05.45.Mt

I. INTRODUCTION

Entanglement is a distinctive feature of quantum mechanics, "*the one that enforces its entire departure from classical lines of thought*" [1]. Its understanding has tremendously progressed in the last decade, due essentially to a vast amount of work regarding the construction and properties of entangled qubits in view of possible applications in quantum information [2]. In a more general context, any dynamical interaction between quantum particles leads to entanglement, which stands as a formidable obstacle to account for the emergence of the classical world. Explaining the unobservability of entanglement in the classical limit is one of the aims of the decoherence program [3].

Somewhat more modestly, several recent works [4–10] have studied in semiclassical systems the link between the generation of entanglement and the dynamics of the corresponding classical system, including in experimental realizations [11]. The numerical and analytical results obtained so far indicate that the entanglement dynamics in quantum systems having a classically chaotic counterpart sharply differs from those whose classical counterpart is regular, though this difference is dependent on the specificities of the considered systems (types and strengths of the coupling, choice of initial states, etc.). It has been argued [12,13] that a proper understanding of the connection between the classical dynamical regime and entanglement hinges on employing systems in which the same physical process generates the dynamics in the classical system and entanglement in its quantum counterpart.

An intriguing question studied in this work concerns the behavior of entanglement in these systems when the typical actions of the system grow with respect to $\hbar$. Then the size of the Hilbert space increases and the quantum-classical correspondence improves. Moreover, if the system dynamics can be kept invariant while the actions increase, an effective Planck constant $\hbar_{\rm eff}$ can be defined and entanglement can be studied as $\hbar_{\rm eff} \to 0$. We will see that entanglement indeed increases with the size of the Hilbert space, in agreement with previous findings on entangled Bose-Einstein condensates [14]. Maybe more surprisingly for sufficiently low $\hbar_{\rm eff}$ is that the evolution of the entanglement measure is given by probabilities obtained from the classical dynamical evolution, irrespective of the dynamical regime.

We start by expounding in Sec. II the quantum system employed as well as its classical counterpart, insisting on the invariance properties which allow fixed dynamics to be studied while varying $\hbar_{\rm eff}$. We then compute in Sec. III entanglement for different values of $\hbar_{\rm eff}$ in the quantum system and investigate the link between entanglement and the classical probabilities (in particular, the classical mutual information). We then discuss (Sec. IV) the meaning of our results, since it appears that as $\hbar_{\rm eff} \to 0$ the quantum information encoded in the pure state density matrix becomes indiscernible from the classical information contained in a mixed density matrix yielding the same reduced dynamics

II. MODEL: A SCATTERING SYSTEM

A. Quantum model

Let us consider bipartite entanglement generated by repeated inelastic scattering of two particles. To set the model, let us assume a light structureless particle and a heavy rotating particle, modeled by a symmetric top with angular momentum N and energy $E_N = N(N+1)/2I$, I denoting the moment of inertia. The scattering potential is taken to be a contact interaction so that the light incoming particle receives a kick when it hits the rotating top. The conservation of the total angular momentum $\mathbf{T} = \mathbf{N} + \mathbf{J}$, where J is the light particle angular momentum, imposes that after the collision the rotating top is left with an angular momentum N' obeying

$$T - J \leqslant N' \leqslant T + J, \tag{1}$$

where we have assumed $J' = J$. The probability of the transition $N \to N'$ is obtained from the scattering matrix elements $|S_{NN'}|^2$. Finally, to account for repeated scattering we need an attractive long-range field between both particles; we assume the particles have opposite electric charge. Note that this model can be seen as a two-particle extension of the standard kicked top well-known in quantum chaos [11,15].

Starting from an initial product state

$$|\psi_0\rangle \equiv |F_0^-(\bar{\epsilon}_0)\rangle |N_0\rangle, \tag{2}$$

where $|F_0^-\rangle$ depicts an incoming wave packet of the light particle with mean energy $\bar{\epsilon}_0$ traveling toward the rotating top in state $|N_0\rangle$, entanglement is generated as soon as the first

collision takes place. The outgoing wave function is then given by the superposition

$$\sum_N S_{NN_0}|F^+(\epsilon_N)\rangle|N\rangle, \tag{3}$$

where the dependence of ϵ on N is due to the conservation of energy, $\epsilon_N = E - E_N$, with $E = \bar{\epsilon}_0 + E_{N_0}$ being the total energy. The scattered wave packets are later turned back by the attractive field and are treated as newly incoming waves. The pure state density matrix

$$\rho(t) = U(t,t_0)|\psi_0\rangle\langle\psi_0|U^+(t,t_0) \tag{4}$$

is obtained by writing the evolution operator U in terms of the scattering eigenstates of the Hamiltonian

$$|\psi(E)\rangle = \sum_N Z_N^-(E)|F^-(\epsilon_N)\rangle|N\rangle + \sum_{NN'} Z_N^-(E)S_{N'N}|F^+(\epsilon_{N'})\rangle|N'\rangle, \tag{5}$$

where Z_N^- are coefficients obtained by applying the asymptotic boundary conditions for closed channels, as is usually done in quantum defect theory [16]. Note that working with closed scattering channels introduces a slight non-Hermitian character to the wave functions [17] that must be taken into account in the numerical computations.

The maximal number of entangled states is given by the number of scattering channels n. This number is obtained from Eq. (1) as $n = 2J + 1$. The amount of entanglement will be estimated through the entropy of the reduced density matrix. We employ the linearized form

$$H(t) = \frac{n}{n-1}\left[1 - \mathrm{Tr}_N \rho_N^2(t)\right], \tag{6}$$

which becomes a good approximation for large n. $\rho_N(t)$ is the reduced density matrix obtained by tracing over the light particle's degrees of freedom. Note $H = 1$ for a maximally entangled state.

For convenience, from this point forward we set $t_0 = \tau_\epsilon/2$, where τ_ϵ is the period of the mean energy orbit; then the collision times are $t = q\tau_\epsilon$ with q being an integer. The system is initially in the product state (2), i.e., in a well-defined channel N_0 with $H(t_0) = 0$. After the first ($q = 1$) collision the system is left in a superposition of states, each of the states being characterized by a symmetric top with an angular momentum N and a light particle with the corresponding energy ϵ_N. Entanglement is therefore generated and $H(t)$ increases.

B. Classical model

The classical version of the model can be formally obtained by employing the semiclassical link [18,19] between the deflection angle ϕ produced by the torsional motion and the eigen-phaseshifts δ of the S matrix. In the top's reference frame, each kick rotates $\mathbf{J}$ by an angle

$$\phi = kJ_\perp/J = \partial\delta/\partial J_\perp, \tag{7}$$

where $J_\perp$ is the projection of $\mathbf{J}$ on the unit axis $\hat{\mathbf{N}}_\perp$ perpendicular to $\mathbf{N}$, and k is the strength of the kick. A given k corresponds, via the semiclassical relation, to a given S matrix, i.e., $S_{NN'} = S_{NN'}(k)$.

The classical orbit of the light particle between two scattering events induces a rotation of $\mathbf{J}$ around $\mathbf{N}$ by an angle $2\pi\tau_\epsilon/\tau_N$, where τ_N is the top rotation period. A surface of section is obtained by plotting the position of $\mathbf{J}$ after each kick [see Figs. 1(b) and 3]. The crucial observation is that the surface of section depends only on k and on τ_ϵ/τ_N: N, J, and T (which are action variables) can be increased at will, say by division by $\hbar_{\mathrm{eff}}$ (a dimensionless constant smaller than 1), but the dynamical map stays constant provided E and I are adjusted accordingly. For a long-range central field this also implies dividing the radial action W_r of the light particle by the same constant $\hbar_{\mathrm{eff}}$.

The classical evolution analog of the quantum problem exposed above is obtained by first discretizing the classical configuration space. This is done by identifying on the Poincaré surface of section the regions corresponding to the quantum density matrices $|N'\rangle\langle N'|$ for the n available quantum states: we cut the sphere along the $\mathbf{N}$ axis into n slices of width $1/n$, each slice being centered so that the projection $J_\parallel$ on the $\hat{\mathbf{N}}_\parallel$ axis corresponds to integer values of N' according to the relation

$$J_\parallel(N') = \mathbf{T}\cdot\hat{\mathbf{N}}_\parallel - N', \tag{8}$$

obtained from the conservation of the total angular momentum. Overall we thus have n intervals $\Delta_{N'} = [N' - \frac{1}{2n}, N' + \frac{1}{2n}]$, with N' being an integer varying within the bounds given by Eq. (1). For a definite classical system the value of N' is obtained by finding the interval $\Delta_{N'}$ to which $J_\parallel(N')$ belongs. Thus the classical distribution corresponding to the initial density matrix $|N_0\rangle\langle N_0|$ is represented on the sphere by the ring centered at $J_\parallel(N_0) = \mathbf{T}\cdot\hat{\mathbf{N}}_\parallel - N_0$. The light particle initial distribution is the same Gaussian employed in the quantum problem; the role of this distribution is to give a statistical weight, depending on the initial energy of the light particle, to each $\mathbf{J}$ lying in the initial ring.

In order to follow the evolution, the position of each $\mathbf{J}$ lying within the initial distribution is computed after each collision (implying a torsion of $\mathbf{J}$ around $\hat{\mathbf{N}}_\perp$ during the kick and a rotation of $\mathbf{J}$ around $\mathbf{N}$ during the orbital excursion). The classical probability $p_N^{\mathrm{cl}}(t = q\tau_\epsilon)$ of finding the top with an angular momentum in the interval $\Delta_N = [N - \frac{1}{2n}, N + \frac{1}{2n}]$ after q kicks is obtained by counting the relative number of vectors $\mathbf{J}$ whose projection falls in the corresponding interval. The probabilities of finding the classical system with the top angular momentum having the value N (i.e., in the interval Δ_N) after the first kick is given by the transition probability $p_N^{\mathrm{cl}}(\tau_\epsilon) = P^{\mathrm{cl}}(\Delta_{N_0} \to \Delta_N)$. The classical probabilities after q kicks are obtained by recurrence from the relation

$$p_N^{\mathrm{cl}}(q\tau_\epsilon) = \sum_{N'} P^{\mathrm{cl}}(\Delta_{N'} \to \Delta_N) p_{N'}^{\mathrm{cl}}[(q-1)\tau_\epsilon]. \tag{9}$$

From these probabilities one can define the quantity

$$M(q\tau_\epsilon) = \frac{n}{n-1}\left[1 - \sum_N \left[p_N^{\mathrm{cl}}(q\tau_\epsilon)\right]^2\right] \tag{10}$$

that can be understood equivalently as the linear entropy for the total system or as the (linearized) classical mutual information, quantifying the amount of mixing induced by

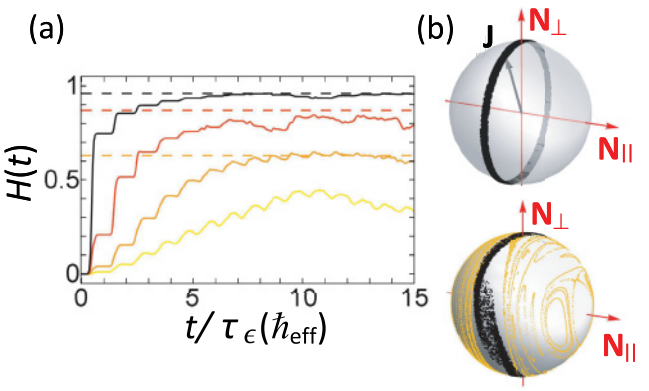

FIG. 1. (Color online) (a) The entanglement rate as a function of the number of kicks is given for quantum systems characterized by $k = 0.25$ and $\hbar_{\rm eff} = 0.5, 0.25, 0.1, 0.01$ (from bottom to top). The dashed lines result from applying the scaling relation (11) to the three upper curves. (b) Top: The black ring encircling the **N** axis is the initial classical distribution of **J** with $J = 10$ (corresponding to the quantum case with $\hbar_{\rm eff} = 0.1$), centered on $N_0 = T = 50$. Bottom: The distribution at $t = 10$ kicks (black dots), showing a spread. The surface of section for $k = 0.25$ is shown in yellow (light gray).

the kicks among the n slices of the discretized classical problem (by doing so the integral over N is separated as $\int_{T-J}^{T+J} \cdots dN = \sum_{\Delta_N} \int_{\Delta_N} \cdots dN$).

III. ENTANGLEMENT AND CLASSICAL PROBABILITIES

A. Entanglement as $\hbar_{\rm eff} \to 0$

We have noted above that the classical dynamics, as it is reflected in the stroboscopic map, is left invariant if all the actions are divided by a small constant provided τ_ϵ/τ_N is left unchanged. This property holds for any value of the coupling k. For the quantum mechanical system, multiplying the quantum numbers N, J, T, and the radial quantum phase counterpart [20] of the radial action W_r by the common factor $1/\hbar_{\rm eff} \gg 1$ is tantamount to studying the limit $\hbar \to 0$ without modifying the dynamics.[1] Indeed, dividing these quantum numbers by $\hbar_{\rm eff}$ can also be seen as multiplying $\hbar$ by $\hbar_{\rm eff}$ (while leaving these numbers unchanged), amounting to introducing an effective Planck constant $\hbar_{\rm eff} \times \hbar$. Then making $\hbar_{\rm eff} \to 0$ allows investigation of the dynamics in the semiclassical regime, in which the quantum evolution is known to be driven by the underlying classical dynamics [21]. Note that the number of channels n (proportional to N) also scales with $1/\hbar_{\rm eff}$.

Figure 1(a) displays the entanglement evolution for the quantum two-particle kicked top with $k = 0.25$ for different values of $\hbar_{\rm eff}$ (we employ atomic units and set $\hbar = 1$). The light particle's initial distribution is a Gaussian wave packet localized far from the symmetric top with its mean initial momentum directed toward it. The entanglement increases dramatically as $\hbar_{\rm eff}$ decreases, despite the fact that the initial state takes a smaller relative area on the sphere. To first order, this is a consequence of the similarity transformation: on the one hand $\rho_N(t)$ is by definition a convex combination of projectors $|N\rangle\langle N|$, and on the other hand in the semiclassical approximation the projection of $\rho_N(t)$ on the unit sphere (at kick times $t = q\tau_\epsilon$) covers the same area irrespective of $\hbar_{\rm eff}$.

Let m be the number of projectors $|N\rangle\langle N|$ (out of total of n) projecting in this area for some $\hbar_{\rm eff}$ and m' that number for another choice of $\hbar'_{\rm eff} < \hbar_{\rm eff}$. Then $m/n = m'/n'$ from which it follows that for situations corresponding to the maximal entanglement (uniform distribution in that region) there is a simple scaling relation for the purity $1 - H$, yielding

$$H'(t) = 1 - \frac{\hbar'_{\rm eff}}{\hbar_{\rm eff}}[1 - H(t)]. \tag{11}$$

As expected entanglement increases with the number of available quantum states.

B. Entanglement and classical mutual information

Figure 2(a)–2(d) shows in the left panel the entanglement evolution as given by $H(t = q\tau_\epsilon)$ for a choice of different

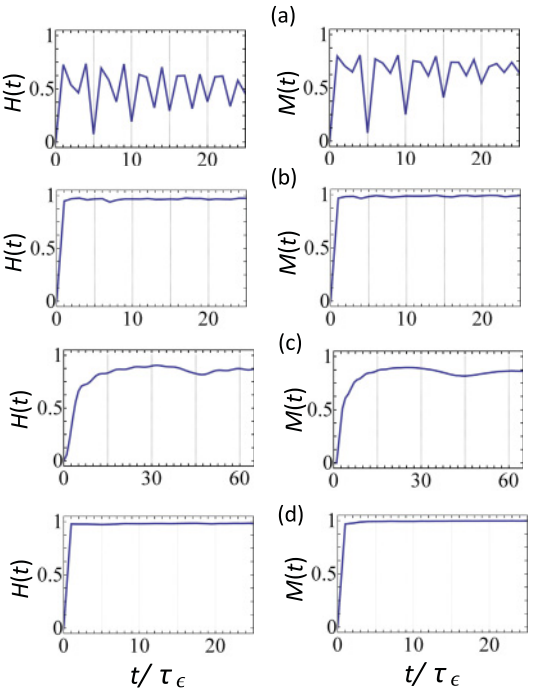

FIG. 2. (Color online) For chosen values of the coupling k and initial state, each row shows on the left-hand side entanglement evolution as computed from the entropy $H(t)$, and on the right the mutual information $M(t)$ of the corresponding classical counterpart. The time t is computed at the discrete kick times $t = q\tau_\epsilon$. The parameters are $J = 100, T = 500$ (corresponding to $\hbar_{\rm eff} = 0.01$ for the quantum system), and (a) $k = 1, N_0 = 402$; (b) $k = 1, N_0 = 430$; (c) $k = 0.01, N_0 = 498$; and (d) $k = 10, N_0 = 460$.

[1]Recall that in general most systems do not have this scaling property; increasing the quantum numbers leads to a different dynamical behavior.

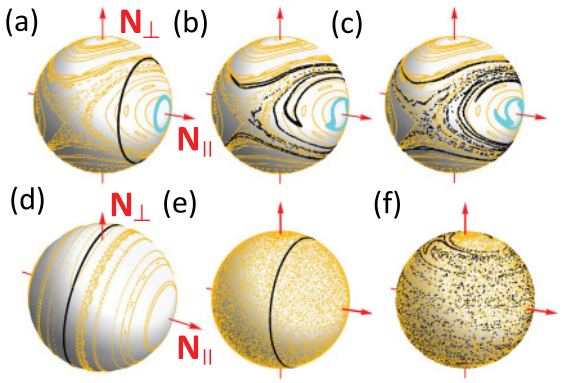

FIG. 3. (Color online) Classical evolution and surfaces of section for the parameters corresponding to the plots of Fig. 2. (a)–(c) For $k = 1$ (mixed phase-space), (a) gives the initial distributions for $N_0 = 402$ [blue (gray) ring] and $N_0 = 430$ (black ring); (b) displays the distributions after ten kicks; (c) at $t = 25$. (d) Position of the initial distribution defined by $N_0 = 498$ for $k = 0.01$ (regular dynamics). (e), (f) Distributions for $k = 10$ (mostly chaotic phase space) and $N_0 = 460$ at $t = 0$ [(e)] and at $t = 5$ kicks [(f)].

system parameters (the coupling k and the initial state are varied) all corresponding to $\hbar_{\rm eff} \approx 1/100$, two orders of magnitude smaller than the hard quantum case $\hbar_{\rm eff} \approx 1$ (which is the typical value for qubits), but still considerably larger than typical values characterizing classical actions. (Note that quantum computations for density matrices become very demanding as $\hbar_{\rm eff}$ decreases, since the dimension of the Hilbert space increases linearly.) The right panel in each plot shows $M(q\tau_\epsilon)$ obtained from the classical probabilities through Eq. (10).

The good agreement between $H(t)$ and the time-dependent classical probabilities holds for classically chaotic and regular regimes alike. In particular, the absence of an oscillating behavior for the linear entropy corresponding to a classically regular regime is noteworthy. The classical surfaces of section corresponding to the parameters (a)–(c) of Fig. 2 are plotted in Fig. 3. Recall that the spread of the distribution along the $\mathbf{N}_\parallel$ axis accounts for the variation of $M(q\tau_\epsilon)$, and hence for the evolution of the entanglement.

C. Linking entanglement with classical probabilities

The results shown in Fig. 2 indicate that entanglement can be quantified by means of classical probabilities. Actually, we expect this behavior to be generic for semiclassical systems that undergo a loss of phase coherence. This is indeed the first ingredient by which the classical $M(q\tau_\epsilon)$ can account for $H(t)$. The second ingredient is the semiclassical approximation itself that allows expression of operator matrix elements in terms of classical quantities (the action and the density of paths). For the system under consideration we start by writing Eq. (5) in the form $|\psi(E)\rangle = \sum_N B_N(E)|F(\epsilon_N)\rangle|N\rangle$, where $|F\rangle$ is a standing wave obtained by combining the $|F^\pm\rangle$ and $B_N(E) \equiv \sum_{N'} S_{NN'} Z^-_{N'}(E) e^{i[W_r^{\rm PO}(\epsilon_N)-\pi]/2}$, and W_r is the radial action of the classical periodic orbit in the attractive field. Then Eq. (4) takes the form[2]

$$\rho(t = q\tau_\epsilon) = \sum_{NN'} |N\rangle\langle N'| e^{-i(E_N - E_{N'})t} \times \beta_N(t)\beta^*_{N'}(t)|F(\bar\epsilon_N)\rangle\langle F(\bar\epsilon_{N'})|, \quad (12)$$

with

$$\beta_N(t) = \sum_{N'} S_{NN'} \left[\sum_E e^{-i\epsilon_N t} Z^-_{N'}(E)\langle\psi(E)|\ \psi_0\rangle \right] \times e^{i[W_r^{\rm PO}(\epsilon_N)-\pi]/2}. \quad (13)$$

(Keep in mind $\epsilon_N = E - E_N$ when taking the sum.) The reduced density matrix is readily derived as $\rho_N(t = q\tau_\epsilon) = \sum_N |N\rangle\langle N| p_N(t)$, with

$$p_N(t = q\tau_\epsilon) = \left|\beta_N\left[t + \frac{\tau_\epsilon}{2}\right]\right|^2 = \left|\sum_{N'} S_{NN'}\zeta^-_{N'}(t)\right|^2. \quad (14)$$

$\zeta^-_{N'}(t)$ is defined by the term between large brackets in Eq. (13) (i.e., by excluding the phase term in the sum). $|\zeta^-_{N'}(t)|^2$ represents the probability on the incoming channel N' just before the collision, whereas $|\sum_{N'} S_{NN'}\zeta^-_{N'}|^2$ is the weight of the outgoing wave right after the collision ($t = q\tau_\epsilon$); in the semiclassical limit this is the same as the weight $|\beta_N|^2$ at the apogee half a period later.[3] It follows that $\zeta^-_N(q\tau_\epsilon) = p_N[(q-1)\tau_\epsilon]$. Finally we recall [18] that in the semiclassical regime the S-matrix elements are given to first order in $\hbar$ by

$$S_{NN'} = \mathcal{A}_{NN'} e^{i\mathcal{S}_{NN'}/\hbar} \text{ with}$$
$$|\mathcal{A}_{NN'}|^2 = P^{\rm cl}(\Delta_{N'} \to \Delta_N), \quad (15)$$

and $\mathcal{S}_{NN'}$ is the classical action. (The boundary conditions for the conjugate momenta obey $p_\theta(t \to -\infty) = N'$ $p_\theta(t \to +\infty) = N$.) In a typical quantum regime, the off-diagonal terms in Eq. (14) produce an oscillating interference pattern that dominates the behavior of the linear entropy. However, as $\mathcal{S}_{NN'}/\hbar \to \infty$ these terms oscillate wildly, while the amplitudes $\mathcal{A}_{NN'}$ are of the same order of magnitude. As a result these off-diagonal terms are suppressed and Eq. (14) becomes

$$p_N(t = q\tau_\epsilon) = \sum_{N'} P^{\rm cl}(\Delta_{N'} \to \Delta_N) p_{N'}[(q-1)\tau_\epsilon]. \quad (16)$$

Comparing with Eq. (9) and given that the initial conditions are identical in the quantum and classical problems, we see that provided the approximations employed hold, the entanglement entropy $H(t = q\tau_\epsilon)$ becomes identical to the mutual information $M(q\tau_\epsilon)$ of the corresponding classical

[2]We assume that the standing-wave dependence on the energy is weak and take the average energy $\bar\epsilon_N$ within each channel, an assumption that holds only for radial positions around the classical outer turning point and thus at times $\tau_\epsilon(q + 1/2)$.

[3]Formally the $\tau_\epsilon/2$ time shift is obtained by applying the radial boundary conditions to Eq. (13) and then expanding $W_r^{\rm PO}(\epsilon_N)$ around $\bar\epsilon_N$ in $|\beta_N|^2$.

system given by Eq. (10), thereby explaining the numerical results displayed in Fig. 2.

D. Quantum discord and classical probabilities

A remarkable consequence of the present results concerns the classical values taken by quantifiers of quantum correlations. For example, the quantum discord $D(\rho)$ [22], widely employed in the context of qubit density matrices, measures the quantum information that can only be extracted by joint measurements on both subsystems. $D(\rho)$ vanishes if the state has only classical correlations. Here $D(\rho)$ is simply given by $H(t)$, hence by the classical mutual information $M(t)$. Put differently, the quantum information contained in the entangled state, which would be the information gained by an observer making a measurement (for example, measuring the light particle's energy ϵ_{N_m} projects the top to the rotational state $|N_m\rangle$), is given by the ignorance spread arising from the dynamical evolution of the corresponding classical system.

Hence as the classical limit is approached the quantum correlations grow, but concurrently, they become increasingly better approximated by statistical distributions of the corresponding classical system. Let $\rho^{\mathrm{CC}}(t) = \sum p_N^{\mathrm{cl}} |N\rangle\langle N||F(\bar{\epsilon}_N)\rangle\langle F(\bar{\epsilon}_N)|$ denote the density matrix containing only classical correlations. The quantum discord is therefore $D(\rho^{\mathrm{CC}}) = 0$. The reduced density matrices obtained from ρ and ρ^{CC} become identical as $\hbar \to 0$. Moreover, the coherences (in the "pointer basis" $|F(\bar{\epsilon}_N)\rangle|N\rangle$) of typical two-particle observables would lead to interference patterns with vanishing (and therefore undetectable) wavelengths [23]. In this sense $\rho(t)$ cannot operationally be distinguished from $\rho^{\mathrm{CC}}(t)$: the effective behavior of the quantum system (that remains highly entangled) becomes classical, and the degree of entanglement can be inferred from the probabilities generated by the evolution of the corresponding classical system.

IV. CONCLUSION

To sum up, we have investigated entanglement evolution when the entanglement is generated by a dynamical localized interaction in a quantum system having a well-defined classical counterpart. The system has an invariance property that allows increasing actions of the system without modifying the dynamics. We have seen that entanglement increases, irrespective of whether the underlying dynamics is regular or chaotic, as typical actions grow relative to $\hbar$. The quantum correlations are then given by the mutual information of the corresponding classical system. This was explained as resulting from the fact that the diagonal approximation holds in the semiclassical regime for sufficiently low values of $\hbar_{\mathrm{eff}}$. When this regime is obtained, although the system is highly entangled, it cannot be distinguished from a classical mixture. The present results could contribute to a better understanding of the role played by quantum information in the classical limit.

[1] E. Schroedinger, Proc. Cambridge Philos. Soc. **31**, 555 (1935).
[2] R. Horodecki *et al.*, Rev. Mod. Phys. **81**, 865 (2009).
[3] W. H. Zurek, Rev. Mod. Phys. **75**, 715 (2003).
[4] R. M. Angelo, K. Furuya, M. C. Nemes, and G. Q. Pellegrino, Phys. Rev. E **60**, 5407 (1999).
[5] J. N. Bandyopadhyay and A. Lakshminarayan, Phys. Rev. Lett. **89**, 060402 (2002).
[6] M. Znidaric and T. Prosen, J. Phys. A **36**, 2463 (2003).
[7] J. Gong and P. Brumer, Phys. Rev. A **68**, 022101 (2003).
[8] M. Lombardi and A. Matzkin, Europhys. Lett. **74**, 771 (2006).
[9] A. M. Ozorio de Almeida, Lect. Notes Phys. **768**, 157 (2009).
[10] Ph. Jacquod and C. Petitjean, Adv. Phys. **58**, 67 (2009).
[11] S. Chaudhury *et al.*, Nature **461**, 768 (2009).
[12] M. Lombardi and A. Matzkin, Phys. Rev. A **73**, 062335 (2006).
[13] C. M. Trail, V. Madhok, and I. H. Deutsch, Phys. Rev. E **78**, 046211 (2008).
[14] R. M. Angelo and K. Furuya, Phys. Rev. A **71**, 042321 (2005).
[15] F. Haake, *Quantum Signatures of Chaos* (Springer, Berlin, 2004).
[16] U. Fano and A. R. P. Rau, *Atomic Collisions and Spectra* (Academic Press, Orlando, FL 1986).
[17] A. Matzkin, J. Phys. A **39**, 10859 (2006).
[18] W. H. Miller, Adv. Chem. Phys. **25**, 69 (1974).
[19] B. Dietz *et al.*, Ann. Phys. **312**, 441 (2004).
[20] A. Matzkin, J. Phys. A **34**, 7833 (2001).
[21] M. Brack and K. Bhaduri, *Semiclassical Physics* (Addision-Wesley, Reading, MA, 1997).
[22] H. Ollivier and W. H. Zurek, Phys. Rev. Lett. **88**, 017901 (2001).
[23] L. E. Ballentine, Phys. Rev. A **70**, 032111 (2004); M. Castagnino *et al.*, Classical Quantum Gravity **25**, 154002 (2008).